Study of Superconductors by Electron Tunneling

IVAR GIAEVER AND KARL MEGERLE
General Electric Research Laboratory, Schenectady, New York
(Received January 3, 1961)

If a small potential difference is applied between two metals separated by a thin insulating film, a current will flow due to the quantum mechanical tunnel effect. For both metals in the normal state the current-voltage characteristic is linear, for one of the metals in the superconducting state the current voltage characteristic becomes nonlinear, and for both metals in the superconductive state even a negative-resistance region is obtained. From these changes in the current voltage characteristics, the change in the electron density of states when a metal goes from its normal to its superconductive state can be inferred. By using this technique we have found the energy gap in metal films 1000–3000 A thick at 1°K to be $2\epsilon_{Pb}=(2.68\pm0.06)\times10^{-3}$ ev, $2\epsilon_{Sn}=(1.11\pm0.03)\times10^{-3}$ ev, $2\epsilon_{In}=(1.05\pm0.03)\times10^{-3}$ ev, and $2\epsilon_{Al}=(0.32\pm0.03)\times10^{-3}$ ev.

The variation of the gap width with temperature is found to agree closely with the Bardeen-Cooper-Schrieffer theory. Furthermore, the energy gap in these films has been found to depend upon the applied magnetic field, decreasing with increasing field.

INTRODUCTION

THE existence of an energy gap in superconductors is well documented experimentally, and is firmly grounded in the theory of superconductivity of Bardeen, Cooper, and Schrieffer.[1] Experimental evidence for the existence of a gap and, indirectly, its width, can be obtained from measurements of specific heat, thermal conductivity, nuclear relaxation, ultrasonic attenuation, and electromagnetic absorption.[2] In general, the width of the gap is inferred from the variation of one of the above parameters and, with the exception of electromagnetic absorption, represents only an indirect measurement.

This paper describes a method for investigating the energy gap and density of electron states in superconductors by means of electron tunneling through thin insulating films. It represents an entirely new approach to the problem and results in clear, unambiguous measurements of the energy gap. Some preliminary results, employing this method, have already been published.[3–6]

The samples used in this experiment consist of a thin insulating oxide layer sandwiched between two evaporated metal films. Experimentally, the electron tunneling current through the insulating oxide layer is observed as a function of the voltage applied between the two metal films. Because of their small physical size, the samples are well suited for standard low-temperature techniques.

If a *small* potential difference is applied to the two metals in their normal, nonsuperconducting state, the tunneling current through the insulating film will vary linearly with applied voltage, as long as the density of electron states in the two metals is constant over the applied voltage range.[7] On the other hand, if the density of electron states varies rapidly in this voltage range, as it does in superconductors, the current-voltage characteristics will be nonlinear. It appears that this nonlinearity is simply correlated with the variation in the density of electron states. In particular, no electrons can flow into the energy region of the gap in superconductors.

By this method we have measured the energy gap in lead, tin, indium, and aluminum. The variation of the energy gap as a function of temperature[6] and magnetic field has also been investigated.

APPARATUS

The apparatus which is shown in Fig. 1 consists basically of a liquid helium Dewar with provisions for

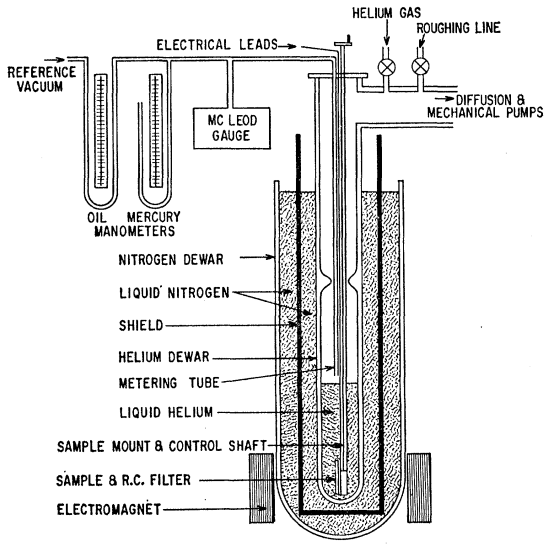

FIG. 1. A schematic drawing of the apparatus. The shield can be removed when studies are made using a magnetic field.

[1] J. Bardeen, L. N. Cooper, and J. R. Schrieffer, Phys. Rev. **108**, 1175 (1957).
[2] M. A. Biondi, A. T. Forrester, M. P. Garfunkel, and C. B. Satterthwaite, Revs. Modern Phys. **30**, 1109 (1958).
[3] I. Giaever, Phys. Rev. Letters **5**, 147 (1960).
[4] I. Giaever, Phys. Rev. Letters **5**, 464 (1960).
[5] J. Nicol, S. Shapiro, and P. H. Smith, Phys. Rev. Letters **5**, 461 (1960).
[6] I. Giaever, Proceedings of the Seventh International Conference on Low-Temperature Physics, Toronto, 1960 (to be published).
[7] J. C. Fisher and I. Giaever, J. Appl. Phys. **32**, 172 (1961).

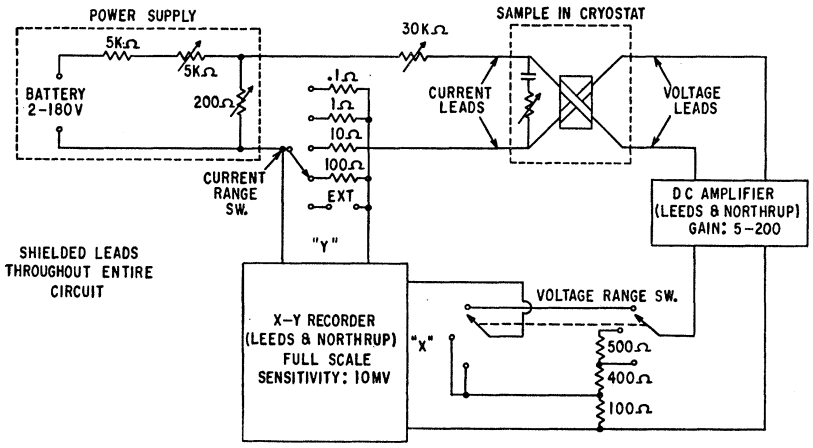

FIG. 2. Circuit diagram of the measuring circuit.

pumping on the helium, and an outer Dewar containing liquid nitrogen which acts as a radiation shield for the helium. The helium Dewar has a constriction in its diameter to minimize creep losses of the superfluid helium when the temperature is below the λ point.

Temperatures are measured by means of the helium vapor pressure. A metering tube which extends to within a few inches of the liquid helium level is connected to both oil and mercury manometers and to a McLeod gauge. The system is capable of attaining a temperature of about 0.9°K. Due to the low heat leakage, this temperature can be maintained for approximately six hours, which is adequate for making numerous measurements.

The electrical circuitry is shown in Fig. 2. To trace out the current-voltage characteristics, a Leeds and Northrup X-Y recorder and matching Leeds and Northrup dc amplifier are used in conjunction with external shunts and multipliers to extend the range of the instruments. These instruments contain chopper-stabilized amplifiers and, therefore, have virtually no drift. To accommodate various sample resistances and to obtain the necessary detail in the current-voltage curves, the current scale can be decade switched over a full-scale sensitivity from 100 ma to 1 μa and the voltage scale from 100 mv to 50 μv.

The emf source can be used as either a high- or low-impedance source, by suitable adjustment of the two variable resistors and the applied battery voltage. The high capacitance of the sample in conjunction with considerable lead inductance gives rise to very troublesome high-frequency oscillations whenever the sample is biased into its negative-resistance region. By placing an adjustable high-pass filter in parallel with the sample, the high-frequency oscillations can be eliminated or at least greatly reduced. The high-pass filter consists of a capacitor large in comparison to the sample capacitance and a variable resistor in series, and is in close proximity to the sample to minimize lead inductance. The oscillations are reduced by matching the variable resistance to the negative resistance of the sample. The variable resistor is a Bourns Trimpot which is mounted on the end of a $\frac{1}{4}\times 0.008$ in. stainless steel tube. Concentric with this tube is a $\frac{1}{8}\times 0.008$ in. stainless steel tube which engages the adjustment screw of the resistor and passes through an O-ring seal in the Dewar cover plate, to permit external adjustments.

The electrical connections into the Dewar, consisting of current and voltage leads, are brought out through the cover plate and are sealed in place with Apiezon wax to achieve a tight seal. In order to minimize heat leaks, four 3-mil Formex-covered copper wires are used inside the cryostat. To minimize induced noise, the entire electrical circuitry outside the Dewar is shielded. The sample and leads within the Dewar can be shielded by a copper-clad soft iron shield which sits in the liquid nitrogen, surrounding the helium Dewar. This shield is not used for measurements made with an externally applied magnetic field.

Since the voltages applied to the sample are very small, induced voltages caused by ever-present fluctuating stray fields remain a difficult problem even after careful shielding. The slow response time of the recording apparatus causes the readings to be averaged over the fluctuations resulting from induced voltages. Due to the nonlinear characteristics of our samples, this averaging tends to smooth out the current-voltage curves and results in lost detail. The difficulty is virtually eliminated by including a resistance in series with the current loop, and making this resistance as large as practical. The large resistance in series with the sample resistance acts as a voltage divider for induced noise, so that only a small amount of noise appears across the sample. This large series resistance effectively increases the emf source impedance and cannot be used when investigating the negative-resistance region of the sample. It has, however, been retained for measurements outside the negative resistance region on most samples.

The sample is mounted directly on the variable resistor which is a part of the high-pass filter. This insures mechanical rigidity and reproducible, accurate positioning for measurements involving magnetic fields.

When the sample is subjected to a magnetic field, it is aligned so that the field vector is in the plane of both films, parallel to the long dimension of the aluminum film, and normal to the long dimension of the other metal film.

SAMPLE PREPARATION

The sample consists of two metal films separated by a thin insulating layer. Aluminum/aluminum oxide/metal sandwiches are prepared by vapor-depositing aluminum on microscope glass slides in vacuum, oxidizing the aluminum, and then vapor-depositing a metal over the aluminum oxide. First the microscope slide is cut to size, $\frac{1}{2}\times 3$ in., so as to fit through the constriction in the helium Dewar. Next, indium is smeared onto the four corners of the glass slide to provide contacts between the evaporated metal strips and external leads. The glass slide with indium contacts is then washed with Alconox detergent, rinsed with distilled water and ethanol, and dried with dry nitrogen gas.

Next, the glass slide is mounted in the evaporator so that it can be positioned behind suitable masks in vacuum. The evaporations are made from tantalum strips approximately $\frac{3}{8}\times 1\frac{1}{2}\times 0.005$ in., which have previously been charged and heated in vacuum so that the charge wets the tantalum strip. The evaporations are made at a starting pressure of 5×10^{-5} mm Hg, or less.

Preparation of the metal/insulator/metal sandwich proceeds in three distinct steps, as shown in Fig. 3, during which the substrate is at room temperature.

First, a layer of aluminum is evaporated onto the glass slide between two contacts. This strip is 1 mm wide and 1000–3000 A thick. Next, the aluminum is oxidized either at atmospheric pressure or some reduced pressure. Finally, a layer of Al, Pb, In, or Sn, of dimensions similar to the aluminum strip, is evaporated over the aluminum oxide layer between the remaining two contacts.

The thickness of the Al_2O_3 insulating layer between the metal strips is subject to a number of variables. The pressure and time dependence of oxidation rate has been extensively investigated and is well documented in the literature.[8] Atmospheric humidity or residual H_2O vapor in the vacuum system also affects the oxidation rate. We have found that an increase in the amount of water effects a more rapid oxide growth rate. The oxide thickness is also contingent upon the evaporation rate and evaporation temperature of the metal layer deposited over the oxide layer. Presumably, metals which require higher temperatures for evaporation must give up more energy to the oxide film; i.e., the atoms penetrate further into the oxide, thereby effectively reducing the thickness of the oxide layer. Another parameter is oxidation temperature, elevated temperatures promoting an increase in the oxidation rate. A final variable is introduced by the evaporation rate of the aluminum layer, which influences its surface characteristics. We have noted that the oxide grows more slowly and reaches a thinner limiting value on films which were evaporated with a high deposition rate (approximately 1000 A/sec).

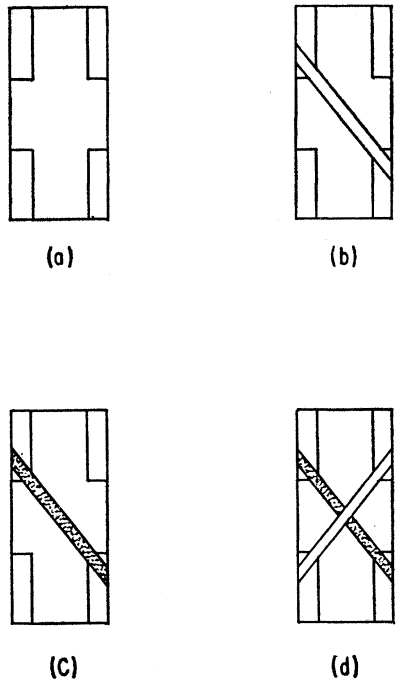

FIG. 3. Sample preparation. (a) Glass slide with indium contacts. (b) An aluminum strip has been deposited across the contacts. (c) The aluminum strip has been oxidized. (d) A lead film has been deposited across the aluminum film, forming an Al-Al_2O_3-Pb sandwich.

TABLE I. Approximate relationship between oxidation time and film resistance for Al-Al_2O_3-Pb sandwiches.

Time	Temperature	Pressure	Resistance (ohm/mm²)
24 hr	100°C	atmospheric	10^5-10^7
24 hr	room	atmospheric	10^3-10^5
10 min	room	atmospheric	$10-10^3$
2 min	room	atmospheric	$1-10^2$
10 min	room	200μ Hg	10^1-10^{-1}
10 min	room	50μ Hg	$10^{-2}-10^{-1}$

By controlling these parameters to some extent, the resistance of a 1-mm² junction can be made to vary between 10^{-2} and 10^7 ohm. Typical oxidation conditions for an Al-Al_2O_3-Pb sandwich are given in Table I. (The resistance variations are probably due to the effect of humidity and the surface characteristics of the aluminum layer.)

It is possible to measure indirectly the thickness of the oxide layer by measuring the capacitance of the junction and then calculating the thickness.[7]

MODEL

The concept that particles can penetrate energy barriers is as old as quantum mechanics. In nuclear

[8] D. D. Eley and P. R. Wilkinson, *Structure and Properties of Thin Films* (John Wiley & Sons, Inc., New York, 1959), p. 508.

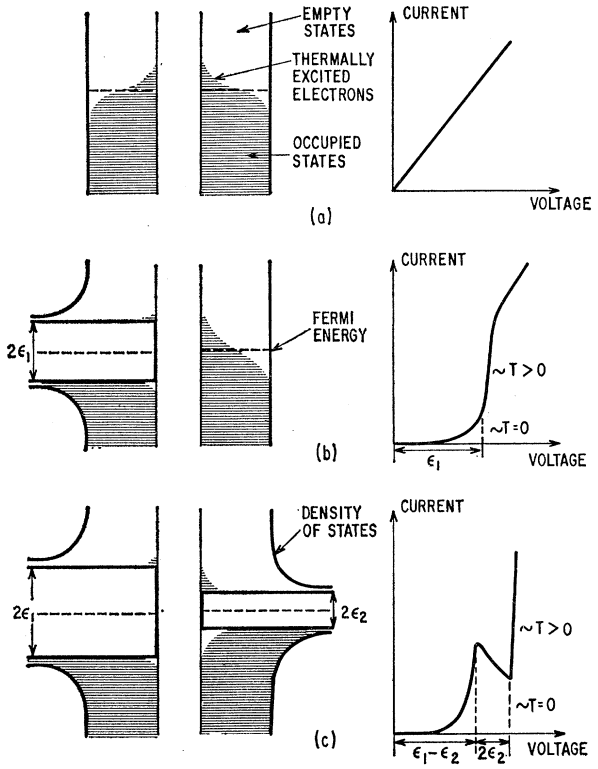

FIG. 4. Energy diagram displaying the density of states and the current-voltage characteristics for the three cases. (a) Both metals in the normal state. (b) One metal in the normal state and one in the superconducting state. (c) Both metals in the superconducting state.

physics, for example, the theory of α decay depends upon this tunnel effect. It has long been known that an electric current can flow between two metals separated by a thin insulating film because of the quantum-mechanical tunnel effect. Theoretical calculations were first made by Sommerfeld and Bethe[9] for a small potential difference applied between the two metals. These calculations were later extended by Holm.[10] An important result of these calculations is that for small voltages across the insulating film the tunnel current through the film is proportional to voltage. Holm *et al.*[11] furnished early experimental evidence for the tunneling effect, a work which was extended by Dietrich[12] and later by Fisher and Giaever.[7] The experiment of tunneling into superconductors[3] furnishes unquestionable evidence that this conduction mechanism is responsible for practically the whole current flow. In the following discussion we shall treat only the low-voltage region where the current flowing through the insulating film is proportional to the voltage across the film, provided both superconductors are in the normal state.

In Fig. 4(a) we show a simple model of two metals separated by a thin insulating film, the insulating film is pictured as a potential barrier. In Fig. 4(b) is shown the case when one of the two metals is in the superconducting state. Note how the electron density of states has changed, leaving an energy gap centered at the Fermi level as postulated by Bardeen, Cooper, and Schrieffer.[1] This particular model of a superconductor is a one-particle approximation, and it gives a surprisingly accurate picture of the experiments. In Fig. 4(c) both the metals are pictured in the superconducting state.

First we shall discuss qualitatively these three different cases, and later quantitatively calculate the current when both metals are in the normal state, and when only one of the metals is in the normal state.

The transmission coefficient of a quantum particle through a potential barrier depends exponentially upon the thickness of the barrier and upon the square root of the height of the barrier. For small voltages applied between the two metals neither the barrier thickness nor the barrier height is altered significantly. The current will then be proportional to the applied voltage, because the number of electrons which can flow increases proportionally to the voltage. The temperature effect will be very small, as the electron distribution is equal on either side of the barrier with metals in the normal state and in addition, kT is much smaller than the barrier height.

When one of the metals is in the superconducting state the situation is radically different. At absolute zero temperature, no current can flow until the applied voltage corresponds to half the energy gap. Assuming that the current is proportional to the density of states, the current will increase rapidly with voltage at first, and then will asymptotically approach the current-voltage characteristic found when both metals were in the normal state. At a temperature different from zero we will have a small current flow even at the lowest voltages. But since the two sides of the barrier now look different, the current will depend strongly upon temperature.

When both metals are in the superconducting state, the situation is again different. At absolute zero no current can flow until the applied voltage corresponds to half the sum of the two energy gaps. At a finite temperature, a current again will flow at the smallest applied voltages. The current will increase with voltage until a voltage equal to approximately half the difference of the two energy gaps is applied. When the voltage is increased further it is possible for only the same number of electrons to tunnel, but since the electrons will face a less favorable (lower) density of states, the current will actually decrease with increasing voltage. Finally, when a voltage equal to half the sum of the two gaps is applied the current will again increase rapidly with voltage and approach asymptotically the

[9] A. Sommerfeld and H. Bethe, *Handbuch der Physik*, edited by S. Flügge (Verlag Julius Springer, Berlin, 1933), Vol. 24, Part 2, p. 333.

[10] R. Holm, J. Appl. Phys. **22**, 569 (1951).

[11] R. Holm, *Electric Contacts* (Hugo Geber, Stockholm, Sweden, 1946).

[12] I. Dietrich, Z. Physik **132**, 231 (1952).

current-voltage characteristics obtained when both metals were normal.

Since we regard the distributions of holes and electrons in the metals in both the normal and superconducting state as symmetric about the Fermi level, no rectification effects are expected.

If we regard the tunneling through the insulating layer as an ordinary quantum-mechanical transition, the transition probability from an occupied state $\mathbf{k}$ on the left side of the barrier to a state $\mathbf{k}'$ on the right side can be written:

$$P_{\mathbf{k}\to\mathbf{k}'}=(2\pi/\hbar)|M|^2n'(1-f'), \tag{4.1}$$

where n' is the density of states on the right side and f' the probability that the state $\mathbf{k}'$ is occupied. $|M|^2$ is the matrix element for the transition and we assume $|M|^2$ vanishes unless the components of $\mathbf{k}$ and $\mathbf{k}'$ transverse to the boundary are equal; that is, specular transmission and then n' is the density of states on the right for fixed wave number components parallel to the boundary. This is a convenient though not an essential assumption.

To calculate the current from left to right we sum over occupied states on the left and obtain

$$i=(4\pi e/\hbar)\textstyle\sum_{k_t}\sum_{k_x}|M|^2n'f(1-f'), \tag{4.2}$$

where k_t is the component of wave number transverse to the barrier, k_x the component perpendicular to the barrier, e the electron charge, and f the probability that state $\mathbf{k}$ is occupied.

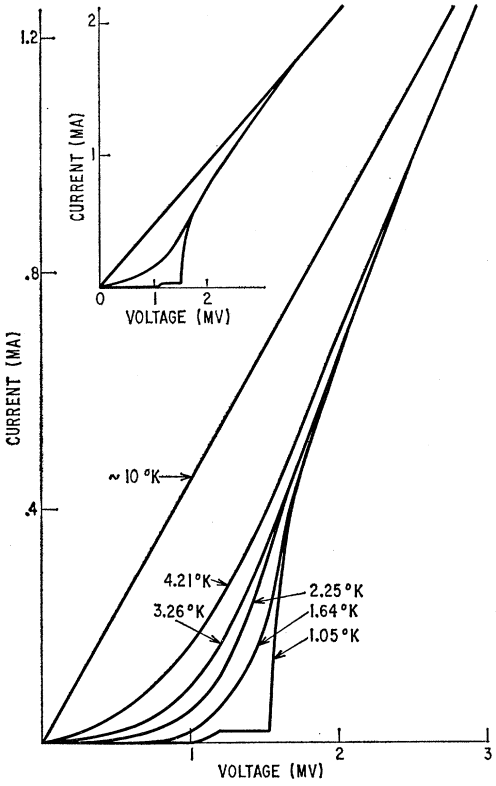

FIG. 5. Current-voltage characteristics of an Al-Al_2O_3-Pb sandwich at various temperatures.

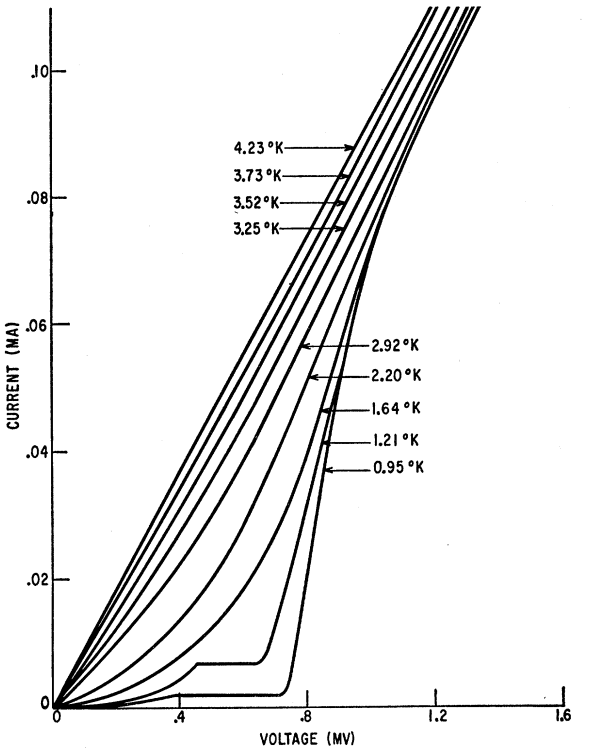

FIG. 6. Current-voltage characteristics of an Al-Al_2O_3-Sn sandwich at various temperatures.

By converting the sum over k_x to an integral over energy with fixed k_t we get

$$i=A\sum_{k_t}\int_{-\infty}^{\infty}|M|^2nn'f(1-f')dE, \tag{4.3}$$

where A is a constant, n the density of states at the left side of the barrier (for fixed k_t), and E the energy measured from the Fermi energy.

By subtracting a similar expression for the current flowing from right to left, we get the net current flow:

$$I=A\sum_{k_t}\int_{-\infty}^{\infty}|M|^2n'n(f-f')dE. \tag{4.4}$$

To fit the experimental results it is necessary to assume that $|M|^2\approx$constant. Bardeen,[13] using a many-particle point of view in connection with the WKB method, finds it plausible that $|M|^2$ is a constant over the energy values of interest. On assuming a constant $|M|^2$ and spherical symmetry of the dependence of energy on wave number, n' and n which are one dimensional densities of states are proportional to the total densities of states, and we may therefore sum over k_t directly and take $|M|^2$ out of the integral. We are

[13] J. Bardeen, Phys. Rev. Letters **6**, 57 (1961).

left with

$$I=A'\int_{-\infty}^{\infty} n'n\{f(E)-f(E+eV)\}dE, \qquad (4.5)$$

where A' is a constant and eV is the difference between the two Fermi levels. (V is the applied voltage.)

For the current between two normal metals we obtain at absolute zero and for small applied voltages:

$$I_{NN}=A'n'(E_F)n(E_F)eV, \qquad (4.6)$$

i.e., the current is proportional to voltage.

For a superconductor we may take the density of states from the Bardeen-Cooper-Schrieffer theory:

$$n_s=n\frac{E}{(E^2-\epsilon^2)^{\frac{1}{2}}}, \qquad (4.7)$$

where E is measured from the Fermi energy, and ϵ is half the energy gap. Thus the current between one metal in the normal state and one metal in the superconducting state can be written:

$$I_{NS}=A'n'(E_F)n(E_F)\int_{-\infty}^{\infty}\frac{|E|}{(E^2-\epsilon^2)^{\frac{1}{2}}}\times[f(E)-f(E+eV)]dE. \qquad (4.8)$$

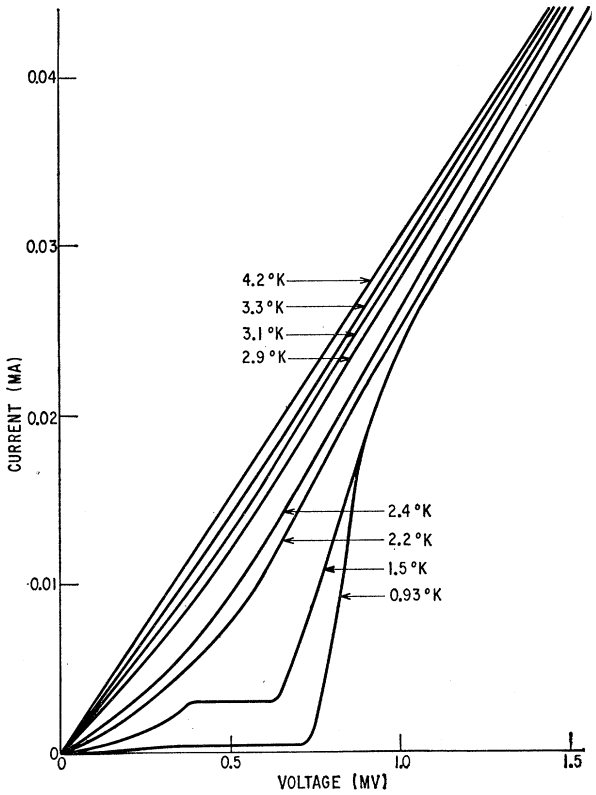

FIG. 7. Current-voltage characteristics of an Al-Al_2O_3-In sandwich at various temperatures.

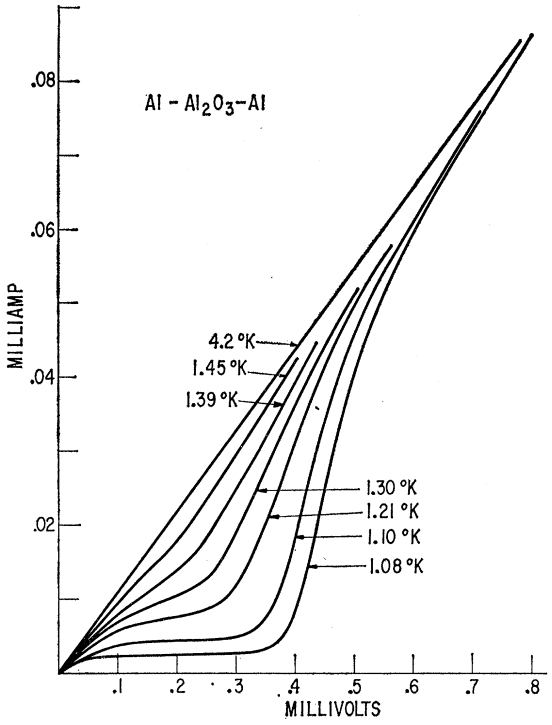

FIG. 8. Current-voltage characteristics of an Al-Al_2O_3-Al sandwich at various temperatures.

For small applied voltages such that $eV<\epsilon$ we may evaluate the above integral, as shown in Appendix I, and obtain:

$$I_{NS}=2C_{NN}\frac{\epsilon}{e}\sum_{m=1}^{\infty}(-1)^{m+1}K_1\left(m\frac{\epsilon}{kT}\right)\sinh\left(m\frac{eV}{kT}\right), \qquad (4.9)$$

where C_{NN} is the conductance when both metals are in the normal state, K_1 is the first order of the modified Bessel function of the second kind, e the electron charge, k the Boltzmann constant, T the temperature, and m an integer. Evaluation of (4.9) for special cases is given in Sec. (c) below. Calculations of the current for $eV>\epsilon$ and for tunneling between two superconductors, require more extensive computation.

Finally, it should be mentioned here that we have treated the insulating layer as if it were a vacuum. However, since the insulator has both a conduction band and a valence band, we could possibly also get a "hole" current. In this particular case this is of little importance as we are mostly interested in the current ratio I_{NS}/I_{NN} rather than the absolute values of current.

EXPERIMENTAL RESULTS

(a) Energy Gaps

We report on four different combinations of superconductors namely Al-Al_2O_3-Pb, Al-Al_2O_3-Sn, Al-Al_2O_3-In,

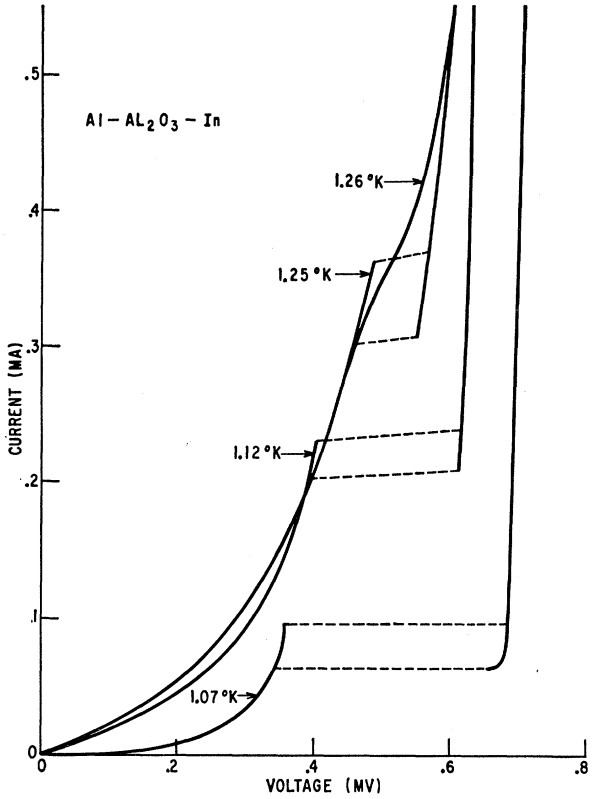

FIG. 9. Detailed current-voltage characteristics of an Al-Al_2O_3-In sandwich, showing the change of energy gap in Al as a function of temperature.

and Al-Al_2O_3-Al. The current-voltage characteristics at various temperatures for these four systems are shown in Figs. 5, 6, 7 and 8, respectively. As seen, the general behavior of the current-voltage characteristics is as predicted from the model. The negative resistance regions are not very apparent on these curves due to the current scale chosen. When the energy gaps on either side of the barrier are equal, as is the case for the Al-Al_2O_3-Al sandwich, a negative resistance region should be observable as well at sufficiently low temperatures. We did not observe this, however, due to temperature limitations in the experimental setup. Note in particular the insert on Fig. 5, showing that for larger voltages the current-voltage characteristics are independent of whether the metals are in the normal or superconducting states. This fact strongly supports the assumption that the tunnel current between superconductors is proportional to the density of states.

From these curves we find the energy gaps at approximately 1°K:

$$2\epsilon_{Pb}=(2.68\pm0.06)\times10^{-3}\text{ ev}=(4.33\pm0.10)kT_c,$$
$$2\epsilon_{Sn}=(1.11\pm0.03)\times10^{-3}\text{ ev}=(3.46\pm0.10)kT_c,$$
$$2\epsilon_{In}=(1.05\pm0.03)\times10^{-3}\text{ ev}=(3.63\pm0.10)kT_c,$$
$$2\epsilon_{Al}=(0.32\pm0.03)\times10^{-3}\text{ ev}=(3.20\pm0.30)kT_c.$$

While the energy gaps in Pb, Sn, and In will not change significantly between 1° and 0°K, this is not true for Al, because of its low transition temperature. It should be noted that the transition temperature for the aluminum films varied from sample to sample, was always greater than the bulk transition temperature, and increased with decreasing thickness of the aluminum films. The highest transition temperature observed for Al was 1.8°K. In calculating the energy gaps in terms of kT_c the bulk transition temperature has been used for all films. One reason for this choice is that the observed energy gap in the aluminum films at 1°K is approximately 0.32×10^{-3} ev, regardless of the transition temperatures observed. This experimental result may be due to the broad transition region usually observed in evaporated films.

(b) Variation of the Energy Gap with Temperature

In Fig. 9 we show detailed current-voltage characteristics for an Al-Al_2O_3-In sandwich as a function of temperature. Because the curves are traced out using a constant current source rather than a constant voltage source, the negative resistance region appears as a hysteresis loop. The width of this loop corresponds ap-

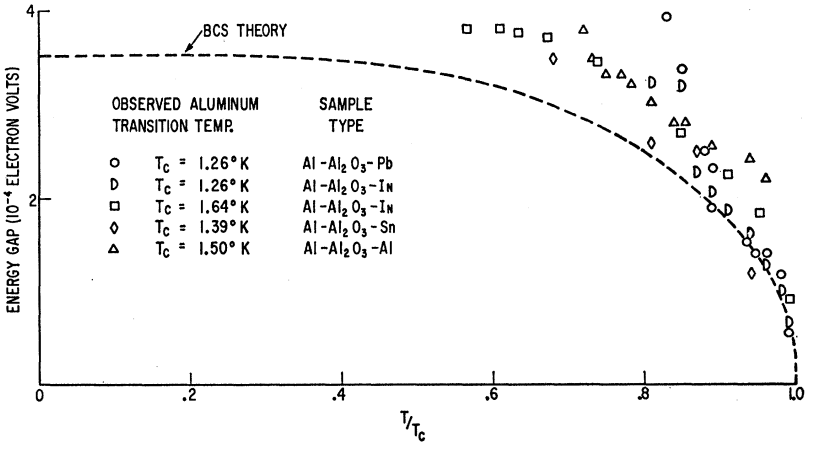

FIG. 10. The energy gap as a function of reduced temperature for several aluminum films, compared with the Bardeen-Cooper-Schrieffer theory.

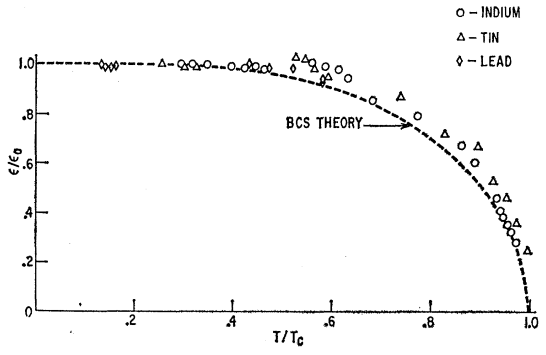

FIG. 11. The energy gap of Pb, Sn, and In films as a function of reduced temperature, compared with the Bardeen-Cooper-Schrieffer theory.

proximately to the full gap width in aluminum, and we can clearly see the variation of gap width with temperature. In Fig. 10 we have plotted the variation of the gap width as a function of reduced temperature for several different samples. For this figure we have used the observed value of the transition temperature T_c. As seen from the figure, the energy gap at $T=0$ does not appear to be very sensitive to the variations in the transition temperature actually observed for the aluminum films. One reason for this could be that the whole area of the aluminum film does not become superconducting at the same temperature, due to localized stresses or impurities. The best estimate of the energy gap for aluminum at absolute zero is

$$2\epsilon_{Al}=(4.2\pm0.6)kT_c=(0.42\pm0.06)\times10^{-3}\text{ ev},$$

where T_c is taken as the bulk value.

It is possible to observe directly the variation of the energy gap in aluminum over the entire applicable temperature range. The energy gap in indium, tin, and lead can also be observed directly in the temperature range in which aluminum is superconducting. At higher temperatures the gap in lead, tin, and indium is not directly observable; however, we are able to calculate the gap width for all temperatures. By letting $V\rightarrow 0$ in Eq. (4.9), we may write:

$$\frac{I_{NS}}{I_{NN}}=2\sum_{m=1}^{\infty}(-1)^{m+1}m\frac{\epsilon}{kT}K_1\left(m\frac{\epsilon}{kT}\right). \qquad (5.1)$$

The quality I_{NS}/I_{NN} as $V\rightarrow 0$ is easily obtained from the experimental results and we may then calculate ϵ from Eq. (5.1). The results are shown in Fig. 11 and are in good agreement with the theory. It should be pointed out that the values of the energy gap, calculated in this way, are in agreement with the directly observed values in the temperature range where both of these measurements can be made. This is most gratifying since these measurements are independent of each other, one being defined at absolute zero, and the other arising solely from the temperature-dependence of the current. The calculated values of the energy gap may appear somewhat too large at low temperatures for some samples due to noise in the measuring circuit.

(c) Calculated versus Measured Current

For tunneling between a metal in the normal state and a metal in the superconducting state, we again use Eq. (4.9) and restrict the calculations to the region where $\epsilon>eV$. In Fig. 12, we compare the calculated values of current with the experimental results obtained on an Al-Al_2O_3-Pb sandwich at various temperatures. The agreement is very good using only two terms of the series in Eq. (4.9). Note in particular that for $\epsilon\gg kT$ and for large voltages such that $\sinh(eV/kT)\approx\frac{1}{2}\exp(eV/kT)$, we may write

$$\ln I_{NS}=\frac{1}{kT}eV+\alpha(\epsilon,T), \qquad (5.2)$$

where α is some function of ϵ and T, independent of V. Thus we can determine the temperature directly from the slope when we plot $\ln I_{NS}$ versus V.

(d) Variation of the Energy Gap with Magnetic Field

By subjecting these samples to a magnetic field parallel to the plane of the metal films, we have found that the energy gap is a function of the applied field. In Fig. 13 we show some detailed results obtained on an Al-Al_2O_3-Pb sandwich. These results are summarized in

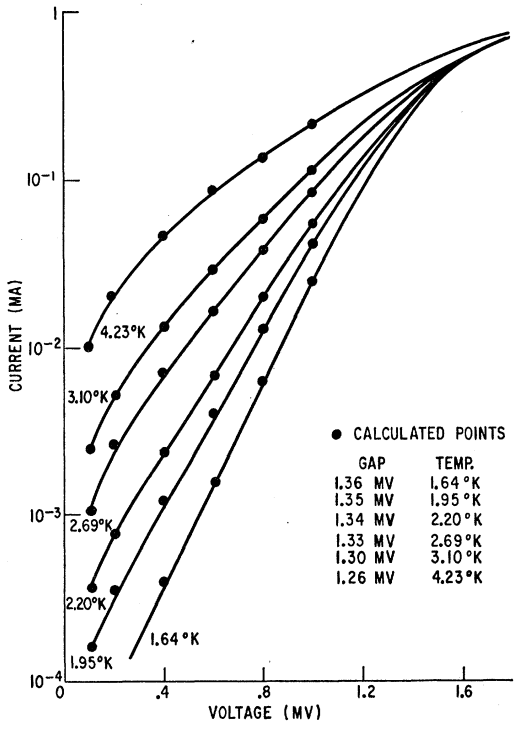

FIG. 12. Observed current-voltage characteristics for an Al-Al_2O_3-Pb sandwich at various temperatures, versus calculated values using the Bardeen-Cooper-Schrieffer density of states.

Fig. 14 where the gap width for aluminum is shown as a function of magnetic field. This curve does not agree with the observed fact that for bulk materials the transition between the normal and superconducting state is a first-order transition. A first-order transition would require a discontinuous change in gap width at the critical field. While this discrepancy may arise from the possibility that the transition is not of first order in a thin film, we believe it more likely that the surface roughness of the film will cause the magnetic field to be nonuniform. This nonuniformity will tend to smear the discontinuous change in gap that we expect at the critical field.

To make sure that the change in the current-voltage characteristics is due to a change in the energy gap, rather than being due to the aluminum film going into the intermediate state, we also investigated the effect of the magnetic field on the energy gap of lead. In Fig. 15 we plot current versus voltage for an Al-Al_2O_3-Pb sandwich at various magnetic fields. If we deal with the intermediate state in lead, then the observed current should be the sum of a current varying linearly with voltage and a current varying exponentially with voltage. This is clearly not so. On the other hand, a good fit to these curves can be obtained by using the expression derived for the tunnel current between one normal and one superconducting member with a varying gap

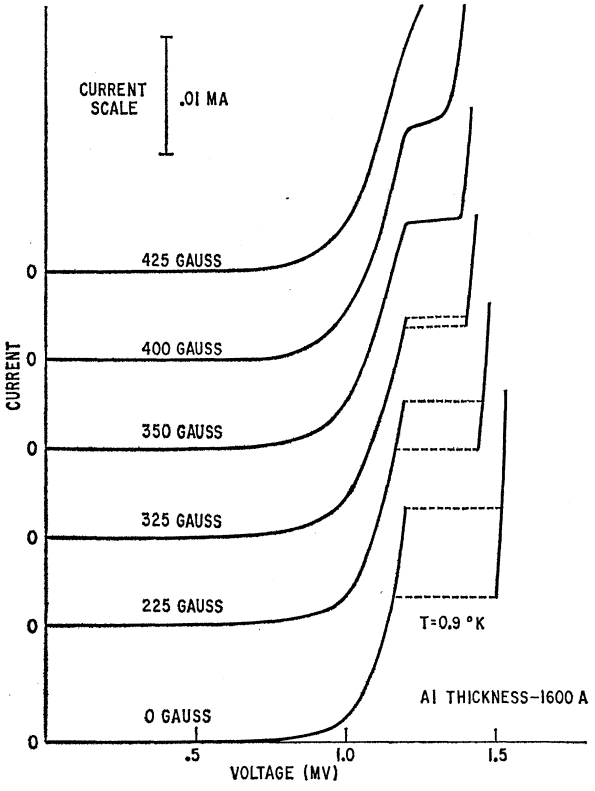

Fig. 13. Detailed current-voltage characteristics of an Al-Al_2O_3-Pb sandwich, showing a change in the energy gap of aluminum as a function of the applied magnetic field.

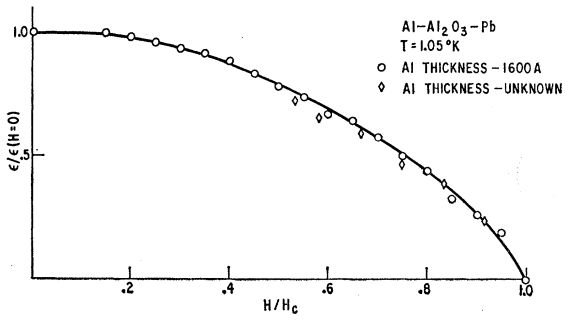

Fig. 14. Apparent variation of the energy gap in an aluminum film as a function of the applied magnetic field.

for different field strengths. To obtain a good fit, it is necessary to use a rather large gap. This is probably due to noise in the measuring circuit or possibly a nonuniform energy gap in lead. It should be mentioned, although no detailed investigation has been made by us, that for thinner films much higher fields are needed to observe the change in the energy gap.

(e) Density of States

The good agreement between the experimental and calculated currents, using the density of states from the

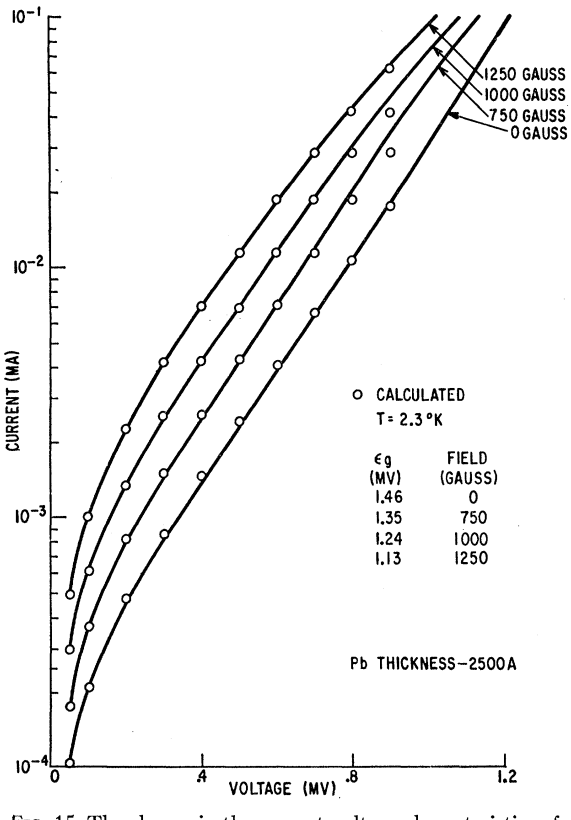

Fig. 15. The change in the current-voltage characteristics of an Al-Al_2O_3-Pb sandwich as a function of the magnetic field, demonstrating that the observed change cannot be due to the lead film being in the intermediate state.

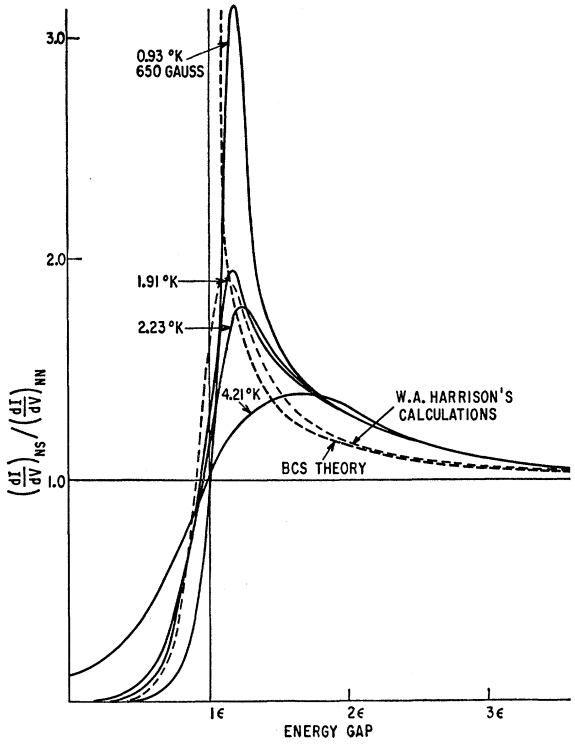

FIG. 16. The relative conductance for an Al-Al_2O_3-Pb sandwich, i.e., the conductance of the sandwich when the lead film is in the superconducting state, divided by the conductance when the lead film is in the normal state, plotted against energy, and compared with the Bardeen-Cooper-Schrieffer density of states. This density of states is used by W. Harrison in his calculations, with $\epsilon/kT=10$.

Bardeen-Cooper-Schrieffer theory, is a great triumph for this theory. In deriving Eq. (4.9), we have integrated over the density of states so that the current is relatively insensitive to small variations in the density of states. Under the assumption that the current is proportional to the density of states, we should get the relative change in the density of states directly by plotting the conductance when one of the metals is superconductive $(dI/dV)_{NS}$ divided by the conductance when both metals are normal $(dI/dV)_{NN}$ against energy. In Fig. 16 we show these results, obtained from an Al-Al_2O_3-Pb sandwich at four different temperatures. Note that at the lowest temperature we have kept the aluminum normal by applying a magnetic field and this again smears the energy gap in lead, making it difficult to assign a specific value to the gap. We see that in spite of the kT smearing, the density of states strongly resembles the theoretical density of states.

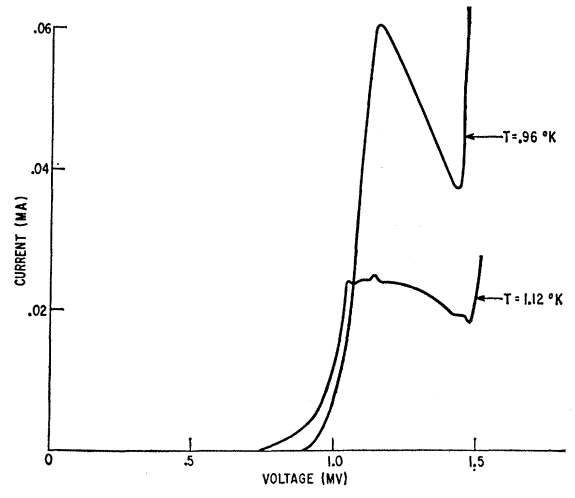

FIG. 17. The negative-resistance region traced out for two different Al-Al_2O_3-Pb sandwiches. We believe the wiggles in the lower curve are due to oscillations in the circuit.

(f) Negative-Resistance Region

In spite of the damping RC network used in parallel with the sample, we found it difficult to eliminate self-induced oscillations in the negative-resistance region. In Fig. 17 we show two attempts to trace out the negative resistance region. We believe that induced noise in the measuring circuit is the limiting factor in tracing out the negative-resistance region, as literally microvolts of induced noise will smear out the curves.

(g) Effect of Metal Bridges and Trapped Flux

In Fig. 18 we show the effect of a metal bridge short-circuiting the sample. The bridge is initially superconducting so that no voltage can be applied across the sample. Then, at a certain current density the bridge becomes normal, but now its resistance is too large to appreciably affect the tunnel current. When the voltage

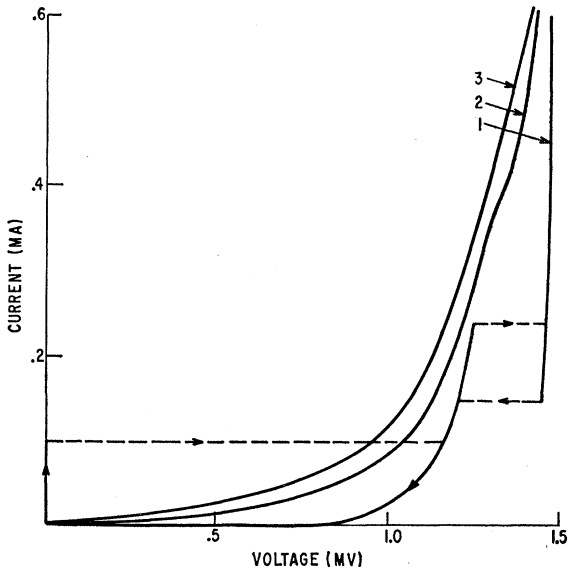

FIG. 18. The effect of trapped flux on the current-voltage characteristic of an Al-Al_2O_3-Pb sandwich. (1) The sample with no field applied; (2) the external field removed, showing the effect of the trapped flux. The figure also shows the effect of a metal bridge across the insulating film; (3) with a magnetic field applied normal to the surface of the films.

is again reduced, the bridge remains normal at a lower current density due to Joule heating.

In Fig. 18 we also show the effect of trapped flux, when the magnetic field purposely has been applied normal to the films. The trapped flux has a large effect upon the current-voltage characteristics, and this technique may possibly be helpful in studying the intermediate state.

(h) Other System

All the experiments we report on have been done by using Al_2O_3 as the insulating layer; however, the experiments may be done by using other insulating layers as well. For example, we have observed tunneling through tantalum and niobium oxides. In these experiments we used bulk specimens of tantalum and niobium; however, we did not observe any evidence for an energy gap in any of these materials. We believe the reason for this is that due to impurities, the surfaces of these materials did not become superconducting. Another superconductor used by us is lanthanum, in which we have observed evidence for an energy gap.

SUMMARY

The method of studying superconductors by electron tunneling has been very successful, and the results are in good agreement with the Bardeen-Cooper-Schrieffer theory. We have directly verified the change of energy gap with temperature. Also, we have shown that for thin films the energy gap is a function of the magnetic field.

ACKNOWLEDGMENTS

We are grateful for the generous and unselfish help received from all members of the Physical Metallurgy Section. We wish to extend special thanks to C. P. Bean, J. C. Fisher, W. A. Harrison, and R. W. Schmitt for their encouragement and interest. Our thanks also to M. V. Doyle for help in performing some of the experiments and L. B. Nesbitt for advice concerning cryogenics.

APPENDIX I

To evaluate the expression:

$$I_{NS}=A'n'(E_F)n(E_F)\int_{-\infty}^{\infty}\frac{|E|}{(E^2-\epsilon^2)^{\frac{1}{2}}}\times[f(E)-f(E+eV)]dE, \quad (A.1)$$

we introduce the conductance C_{NN} when both metals are normal, i.e.,

$$\frac{I_{NN}}{V}=C_{NN}=A'n'(E_F)n(E_F)e, \quad (A.2)$$

and split the integral into two parts:

$$I_{NS}=\frac{C_{NN}}{e}\int_{+\epsilon}^{\infty}\frac{E}{(E^2-\epsilon^2)^{\frac{1}{2}}}\{f(E)-f(E+eV)\}dE - \frac{C_{NN}}{e}\int_{-\infty}^{-\epsilon}\frac{E}{(E^2-\epsilon^2)^{\frac{1}{2}}}\{f(E)-f(E+eV)\}dE. \quad (A.3)$$

By introducing $x+\epsilon=E$ in the first integral and $x+\epsilon=-E$ in the second integral, we get

$$I_{NS}=\frac{C_{NN}}{e}\int_{0}^{\infty}\frac{x+\epsilon}{[(x+2\epsilon)x]^{\frac{1}{2}}}[f(x+\epsilon)-f(x+\epsilon+eV)]dx + \frac{C_{NN}}{e}\int_{\infty}^{0}\frac{x+\epsilon}{[(x+2\epsilon)x]^{\frac{1}{2}}}\times\{f[-(x+\epsilon)]-f[eV-(x+\epsilon)]\}dx, \quad (A.4)$$

and because the Fermi function is an even function,

$$I_{NS}=\frac{C_{NN}}{e}\int_{0}^{\infty}\frac{x+\epsilon}{[(x+2\epsilon)x]^{\frac{1}{2}}}\times[f(x+\epsilon-eV)-f(x+\epsilon+eV)]dx. \quad (A.5)$$

By expanding the Fermi function in a series valid for $\epsilon>eV$, we obtain

$$I_{NS}=2\frac{C_{NN}}{e}\sum_{m}(-1)^{m+1}e^{-m(\epsilon/kT)}\sinh(meV/kT)\times\int_{0}^{\infty}\frac{x+\epsilon}{[(x+2\epsilon)x]^{\frac{1}{2}}}e^{-m(x/kT)}dx. \quad (A.6)$$

The last integral is of a known Laplace-integral form [A. Erdélyi, *Table of Integral Transforms* (McGraw-Hill Book Company, Inc., 1954)], and we obtain

$$I_{NS}=2C_{NN}\frac{\epsilon}{e}\sum_{m}(-1)^{m+1}K_1(m\epsilon/kT)\sinh(meV/kT), \quad (A.7)$$

where K_1 is the first-order modified Bessel function of the second kind.

APPENDIX II

Note added in proof. It is of interest to compare the values of the energy gaps obtained by using electron tunneling to previous direct measurements of the energy gap (Table II).

TABLE II.

Superconductor	Tunneling measurements	Energy gap in units of kT_c: Richards and Tinkham[a]	Ginsburg and Tinkham[b]
Indium	3.63±0.1	4.1±0.2	3.9±0.3
Tin	3.46±0.1	3.6±0.2	3.3±0.2
Lead	4.33±0.1	4.1±0.2	4.0±0.5

[a] P. L. Richard and M. Tinkham, Phys. Rev. 119, 581 (1960).
[b] D. M. Ginsburg and M. Tinkham, Phys. Rev. 118, 990 (1960).